

International Journal of Modern Physics: Conference Series
© World Scientific Publishing Company

Electroweak measurements from W , Z and photon final states

Hang Yin

(On behalf of ATLAS, CDF, CMS, D0, and LHCb collaborations)

*Fermi National Accelerator Laboratory,
Pine Street and Kirk Road, MS 357,
Batavia, Illinois, 50510
yin@fnal.gov*

Received February 26, 2014

Revised Day Month Year

We present the most recent precision electroweak measurements of single W and Z boson cross section and properties from the LHC and Tevatron colliders, analyzing data collected by ATLAS, CDF, CMS, D0, and LHCb detectors. The results include the measurement of the single W and Z boson cross section at LHC, the differential cross section measurements, the measurement of W boson mass, the measurement of W and Z charge asymmetry. These measurements provide precision tests on the electroweak theory, high order predictions and the information can be used to constraint parton distribution functions.

Keywords: LHC, Tevatron, Electroweak, W , Z

1. Introduction

The precision electroweak measurements provide stringent tests the on Standard Model (SM): the measurement of single W and Z boson cross section provides critical tests on the perturbative QCD and the higher order predictions, the measurement of W charge asymmetry can be used to constraint the parton distribution functions (PDFs), and the measurement of W mass and weak mixing angle ($\sin^2 \theta_W$) improves precision of the SM input parameters.

Recently, in both LHC and Tevatron, there are plenty of analyses related to the single W and Z boson have been performed. The LHC is a pp collider, results reviewed in this article used the collision data at center-of-energy of 7 TeV and 8 TeV, collected by the ATLAS¹, CMS² and LHCb³ detectors. The Tevatron is a $p\bar{p}$ collider, with center-of-energy of 1.96 TeV, using data collected by the CDF⁴ and D0⁵ detectors. The W and Z precision measurements have been performed based on these data.

At the Tevatron, the W and Z are produced with the *valence quark*. And at the LHC, in the productions of single W and Z boson, the *sea quark* and *gluon* contributions become larger. Thus, single W and Z measurements at the Tevatron are complementary to that at the LHC. Furthermore, with knowing incoming *quark*

2

direction, the Z forward-backward charge asymmetry at the Tevatron will be more sensitive compared with that measurement at the LHC.

In this article, we review the W and Z cross section measurements from the LHC at first, then review the measurements of boson transverse momentum from both the Tevatron and LHC. In the end, the measurement of the W boson mass, W/Z charge asymmetry measurements, are presented. The physics results are collected from ATLAS, CDF, CMS, D0, and LHCb collaborations.

2. The W and Z total cross section measurements

Precise determination of the vector boson production cross section and their ratios provide an important test of the SM.

2.1. Inclusive cross section

At the LHC, the production of vector boson requires at least one sea quark, and given the high scale of this process, the gluon contribution becomes significant. Furthermore, the inclusive cross section of vector boson production is also sensitive to the PDFs, the cross section predictions depend on the momentum distribution of the gluon. And the theoretical uncertainty is another limitation for the cross section measurement, the current available predictions are at next-to-leading (NLO) and next-to-next-to-leading order (NNLO) in perturbative QCD. In Fig. 1, the measured W and Z cross sections from different hadron colliders are compared with NNLO predictions, the predictions agree with measured value well.

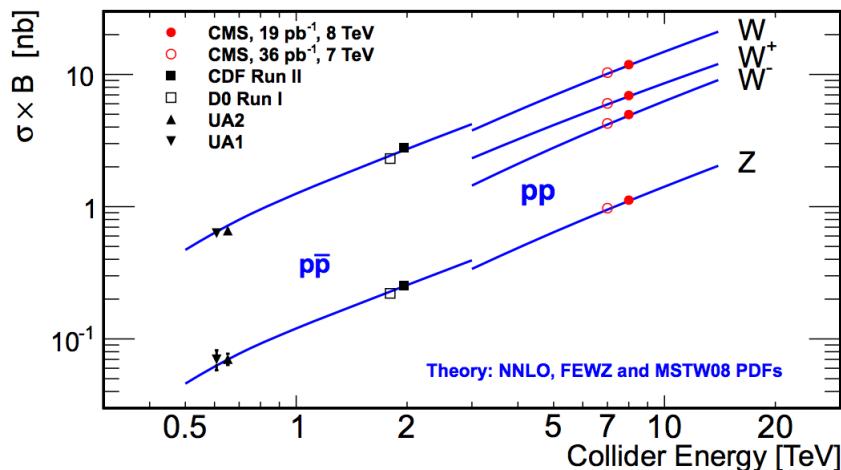


Fig. 1. The inclusive W and Z production cross section times branching ratios as a function of center-of-mass energy measured from CMS and other lower-energy colliders. The blue lines represent the NNLO theory predictions..

Both ATLAS ⁶ and CMS ⁷ collaborations presented the inclusive W and Z cross section at $\sqrt{s} = 7$ TeV, with electron and muon decay channels, using a data sample corresponding to 35 pb^{-1} and 36 pb^{-1} of integrated luminosity collected in 2010. And furthermore, CMS ⁸ using data corresponding to 19 pb^{-1} of integrated luminosity collected in 2012 at $\sqrt{s} = 8$ TeV.

With $\sqrt{s} = 7$ TeV data, the measured inclusive cross sections from CMS are $\sigma(pp \rightarrow WX) \times B(W \rightarrow l\nu) = 10.30 \pm 0.02(\text{stat.}) \pm 0.10(\text{syst.}) \pm 0.10(\text{th.}) \pm 0.41(\text{lumi.})$ nb and $\sigma(pp \rightarrow ZX) \times B(Z \rightarrow l^+l^-) = 0.974 \pm 0.007(\text{stat.}) \pm 0.007(\text{syst.}) \pm 0.018(\text{th.}) \pm 0.039(\text{lumi.})$ nb, and from ATLAS are $\sigma(pp \rightarrow WX) \times B(W \rightarrow l\nu) = 10.207 \pm 0.021(\text{stat.}) \pm 0.121(\text{syst.}) \pm 0.347(\text{th.}) \pm 0.164(\text{lumi.})$ nb and $\sigma(pp \rightarrow ZX) \times B(Z \rightarrow l^+l^-) = 0.937 \pm 0.006(\text{stat.}) \pm 0.009(\text{syst.}) \pm 0.032(\text{th.}) \pm 0.016(\text{lumi.})$ nb.

By presenting the measured cross section as a ratio will result a cancellation of systematic uncertainty, including the luminosity uncertainty. Thus, the ratios between measured W^\pm and Z , also the ratio between W^+ and W^- , are shown in Fig. 2 and Fig. 3.

The measurements of vector boson production cross section are consistent between the electron and muon channels, and in agreement with NNLO order predictions.

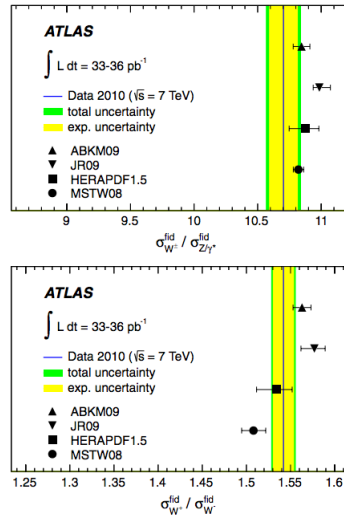


Fig. 2. The ratios between the measured inclusive cross section of W^\pm and Z (top panel), and ratio between the measured inclusive cross section of W^+ and W^- (bottom panel). The inner bands represent experimental uncertainty, and outer bands represent total uncertainty. The PDFs uncertainties from the ABKM, JR, and MSTW predictions are considered in 68% C.L. The HERAPDF predictions include all three sources of uncertainty of that set.

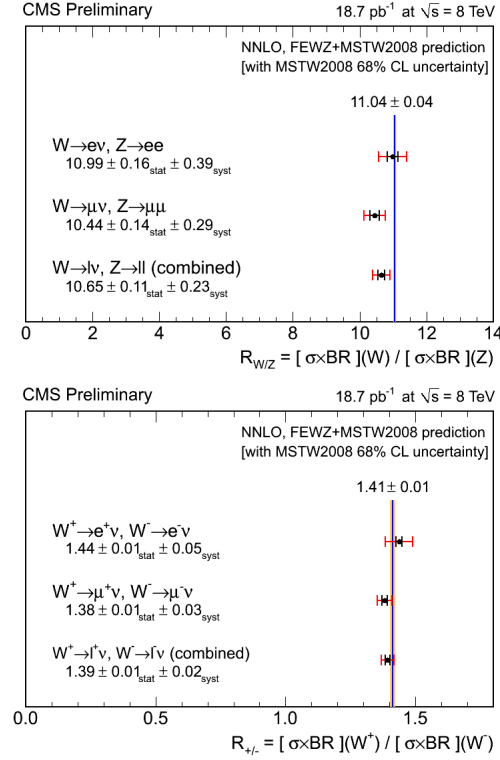


Fig. 3. The ratios between the measured inclusive cross section of W^\pm and Z (top panel), and ratio between the measured inclusive cross section of W^+ and W^- (bottom panel). The black bars represent the statistical uncertainties, while the red errors bars include systematic uncertainties. Measurements in the electron and muon channels, and combined, are compared to the theoretical predictions using FEWZ and the MSTW2008 PDF set.

2.2. Differential cross section

The differential cross section of Drell-Yan (DY) process as a function of two leptons invariant mass is sensitive to the PDFs, particular in the high mass region (corresponding to the distribution function of antiquarks with high x value), and also provide stringent test on the high order perturbative QCD calculations. Additionally, this process is a important source of background for other beyond SM searches, the mass spectrum could be changed by new physics phenomena. The ATLAS⁹ and CMS¹⁰ report measurement of the high mass DY differential cross section measurement, as shown in Fig. 4. The measured differential cross sections are constant with different NLO (or NNLO) theoretical predictions, with more data in the future, this measurement could be used to constraint PDFs, in particular for antiquarks with large x .

CMS also performed a double-differential cross sections measurement¹⁰, as func-

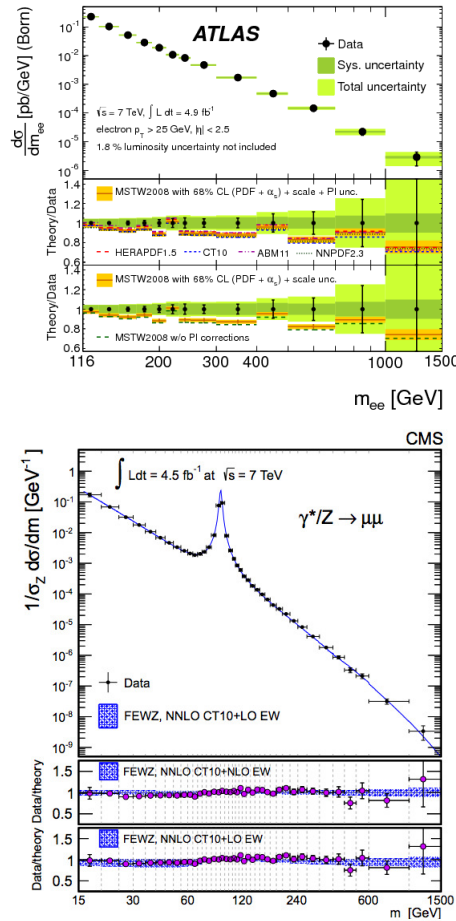


Fig. 4. Measured differential cross section as a function of invariant mass, from ATLAS (top panel) and from CMS (bottom panel). The measured differential cross sections are compared with plenty of high order predictions with different PDF sets.

tions of boson rapidity (y) and invariant mass. By including additional boson rapidity information (y), the differential cross section provides more information for the PDFs, while the low mass region, the high order effects and final state radiation (FSR) become particularly important. The measured differential cross section as a function of boson y in the mass region of 20 to 30 GeV is shown in Fig. 5. The double -differential cross section measurement of DY will provides precise inputs to the future PDF sets fitting.

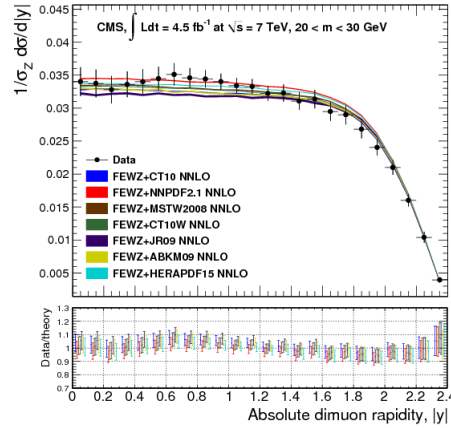


Fig. 5. The measured differential cross section as a function of boson y , in the mass region of 20-30 GeV. The uncertainty bands in the theoretical predictions represent the statistical uncertainty. The bottom plot shows the ratio of measured value to theoretical predictions.

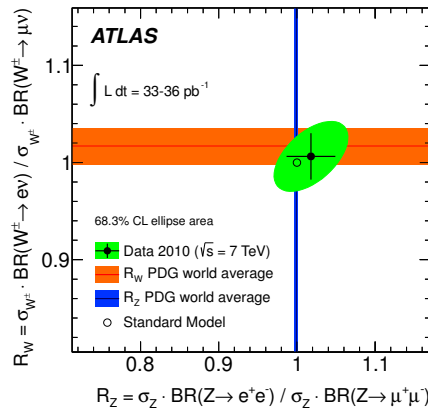


Fig. 6. The correlated measurement of the electron to muon cross section ratios in W and Z events. The vertical band represents the uncertainty from the Z measurement, and the horizontal band represents the uncertainty from the W measurement. The contour illustrates the 68% C.L. for the correlation between W and Z measurements.

2.3. Lepton universality

The coupling of the leptons (e, μ, τ) to the gauge vector boson are independent. The ATLAS performed a measurement of lepton universality⁶, by comparing the cross sections measured using electron channel and muon channel. The ratio between electron and muon channels results is shown in Fig. 6. The result confirms e - μ universality in both W and Z decays.

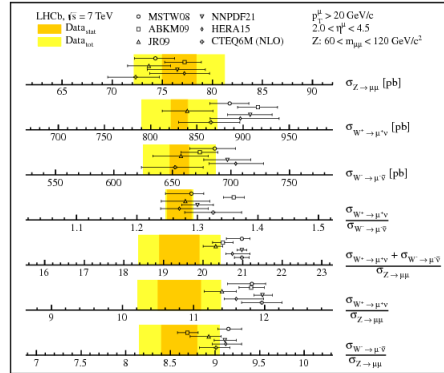


Fig. 7. Measurements of the Z , W^+ and W^- cross-section and ratios from LHCb, data are shown as bands which the statistical (dark shaded/orange) and total (light hatched/yellow) errors. The measurements are compared to NNLO and NLO predictions with different PDF sets for the proton, shown as points with error bars. The PDF uncertainty, evaluated at the 68% confidence level, and the theoretical uncertainties are added in quadrature to obtain the uncertainties of the predictions.

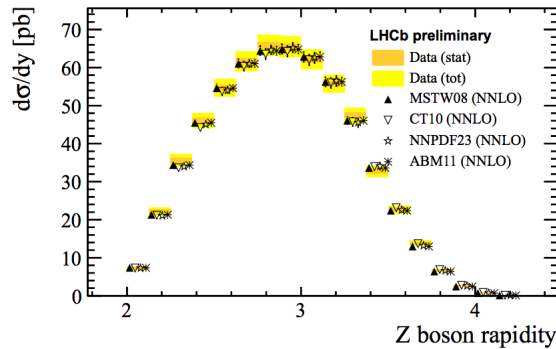


Fig. 8. Differential cross section measurement as a function of Z rapidity at LHCb. The yellow band represent the measured data value, while the NNLO predictions are shown as points with error bars reflecting the uncertainties.

2.4. W and Z cross section measurements at LHCb

In the LHCb, the measurement of the W and Z cross section provide a unique test on the SM with high rapidity W and Z events. Thus, the LHCb results have better precision than ATLAS and CMS in the forward region ($2.0 < \eta < 5.0$). The most recent results^{11,12,13,14} are for the inclusive cross section measurements, and the differential cross section measurement in different channels, as functions of rapidity or invariant mass. The LHCb inclusive cross section measurements results are shown in Fig. 7, and one of the differential cross section measurement from LHCb is shown in Fig. 8.

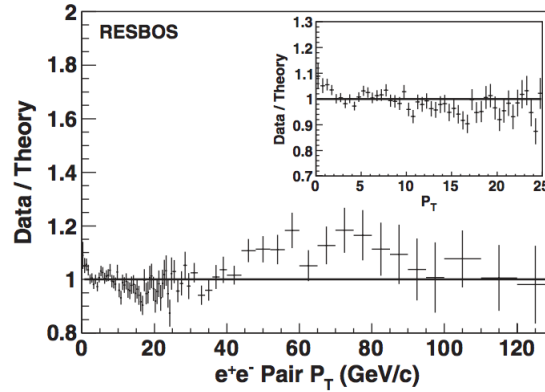


Fig. 9. The ratio of the measured cross section to the RESBOS prediction in the $p_T < 130$ GeV/ c region. The RESBOS total cross section is normalized to the data. The insert is an expansion of the low p_T region.

3. The boson transverse momentum measurements

Initial state QCD radiation from the colliding parton can change the kinematic of the Drell-Yan process system, results Z boson be boosted with a transverse momentum, thus the precision measurement of Z boson p_T can provide a stringent test on the higher order QCD perturbative calculation. And this measurement can be used to reduce the theory uncertainty of the measurement of W mass. In the low p_T region, this process is dominated by soft and collinear gluon emission, with the limitation of standard perturbative calculation, the QCD resummation methods are used in the low p_T region. While in the high p_T region, the process is dominated by single parton emission, thus, fixed-order perturbative calculations are used in the high p_T region.

3.1. Traditional method

In general, the boson p_T can be directly measured by using the reconstructed boson p_T . As has been done before¹⁵, CDF performed a precision measurement of transverse momentum cross section of e^+e^- pairs in the Z -boson mass region of 66-116 GeV/ c^2 , with 2.1 fb⁻¹ of integrated luminosity¹⁶. Fig. 9 shows the ratio between measured data value and RESBOS predictions. And CMS reported a similar measurement using data corresponding to 18.4 pb⁻¹ of integrated luminosity¹⁷, as shown in Fig. 10. The overall agreement with predictions from the SM is observed, and the results have sufficient precision for the refinements of phenomenology in the future.

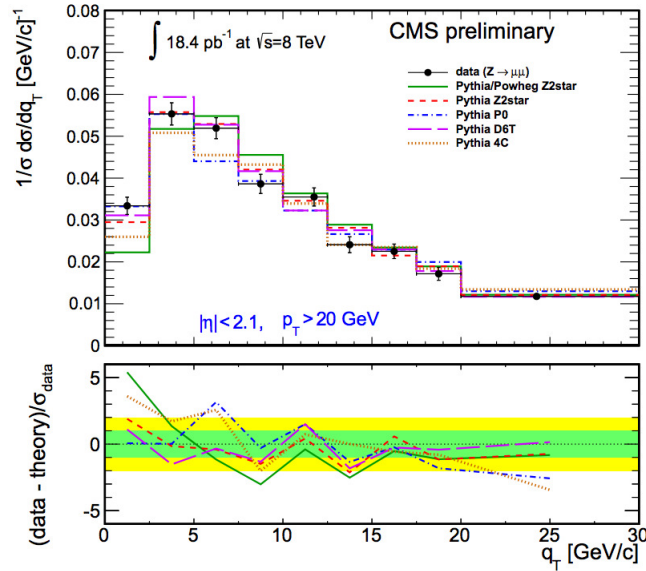


Fig. 10. The transverse momentum distribution of Z boson measurement from CMS. The measure values (black points) are compared with different predictions. In the bottom portion, the difference between data and prediction divided by the uncertainty of data is shown, with the green (inner) and yellow (outer) bands represent the 60% and 90% C.L. experimental uncertainties.

3.2. A Novel method

In the previous Z p_T measurements, the uncertainty is dominated by the experimental resolution and efficiency, and the choice of bin widths is limited by the experimental resolution rather than event statistics. In order to improve the precision of the boson p_T measurements, D0 published measurement of Z boson p_T ¹⁸, presented with a novel variable (ϕ^*) ¹⁹. The ATLAS and LHCb performed same measurements of ϕ^* ^{20,12}, as shown in Fig. 11 and Fig. 12. The measured results provide sufficient information to the future retuning of theoretical predictions.

4. The W and Z properties measurements

There are many other electroweak measurements from Tevatron and LHC, which measure input parameters of the SM with better precision, including the measurement of W mass, the measurement of W charge asymmetry, and the measurement of weak mixing angle.

4.1. Measurement of the W boson mass

The precision measurement of W mass contribute to the understanding of the electroweak interaction. By combining the more recent measurement of W mass from

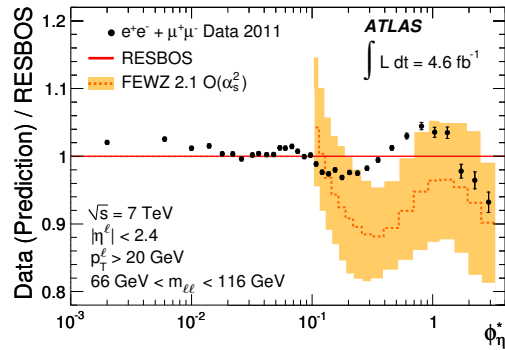


Fig. 11. The ratio of the combined normalized differential cross section to RESBOS predictions as a function of ϕ^* . The inner and outer error bars on the data points represent the statistical and total uncertainties, respectively. The measurements are also compared to predictions, which are represented by a dashed line, from FEWZ 2.1. Uncertainties associated to this calculation are represented by a shaded band.

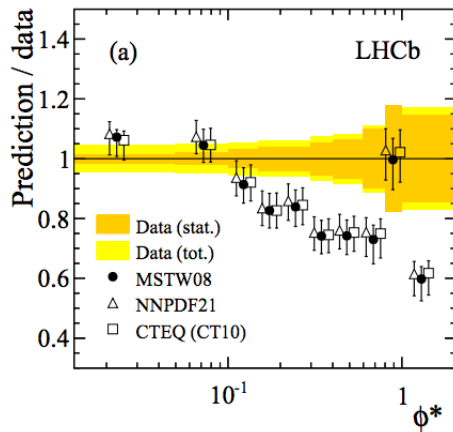


Fig. 12. Ratio of various QCD predictions to the measured data values as a function of ϕ^* , using LHCb data. The NNLO QCD predictions to the measured data are shown in black points.

both CDF ²¹, D0 ²², and previous Tevatron measurements, the Tevatron average value is 80387 ± 16 MeV ²³. The combination of W mass with the LEP average further reduces the uncertainty to 15 MeV, as shown in Fig. 13.

4.2. W charge asymmetry measurements

The W charge asymmetry is sensitive to PDFs. The Tevatron is a $p\bar{p}$ collider, the u quark tends to carry higher momentum than d quark, thus arise a non-zero asymmetry as a function of W rapidity. The LHC is pp collider, proton has two valance u

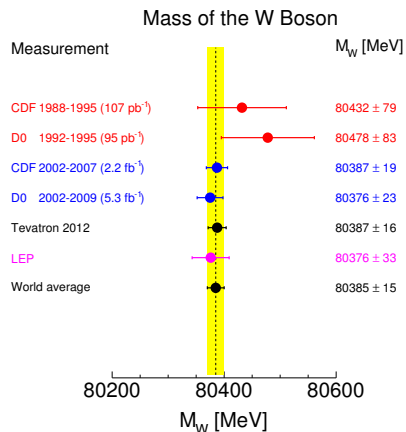


Fig. 13. Measured W boson mass from the CDF and D0 Run I (1989 to 1996) and Run II (2001 to 2009), the new Tevatron average, and the LEP combined results, and the world average obtained by combining the Tevatron and LEP measurements, with assumption that no correlation between them. The shaded band is the new world-average uncertainty (15 MeV).

quarks and one valence d quark, there are more W^+ than W^- . In hadron colliders, the neutrino escapes the detector without producing any measurable signal, without the neutrino longitudinal momentum, the W charge asymmetry can be measured as lepton charge asymmetry, which is a convolution of the W boson asymmetry and W V - A decay.

The lepton asymmetry has also been measured at the LHC in pp collisions by the ATLAS²⁴ and CMS^{25, 26} Collaborations using data corresponding to 31 pb⁻¹ and 840 pb⁻¹ of integrated luminosity, respectively. One of CMS results is shown in Fig. 14. With 37 pb⁻¹ of integrated luminosity collected with LHCb detector, the lepton charge asymmetry is performed using muon channel¹¹, as shown in Fig. 15. These measurements provide useful information for future PDF set fitting.

4.3. Weak mixing angle measurements

Weak mixing angle is one of fundamental parameters in the SM. It is one of key input parameters related to the electroweak couples, for both charge current (W) and neutrino current (Z). The weak mixing angle is a running parameter in a wide region of center-of-energy, there are many measurements have been done at the low energy experiments, like atomic parity violation²⁷, Møller scattering²⁸, and NuTeV²⁹. In the Z peak region, the most precision measurements are from LEP b quark asymmetries, and SLD Left-Right hand asymmetries (A_{LR})³⁰. The results from LEP and SLD are deviated by three standard deviations in different directions.

Recently at the hadronic collider, CDF³¹, D0^{32,33}, and CMS^{34,35} have been performed this measurement, which show reasonable agreement with world average value. Due to the limitations from PDFs and quark fragments, the dominated

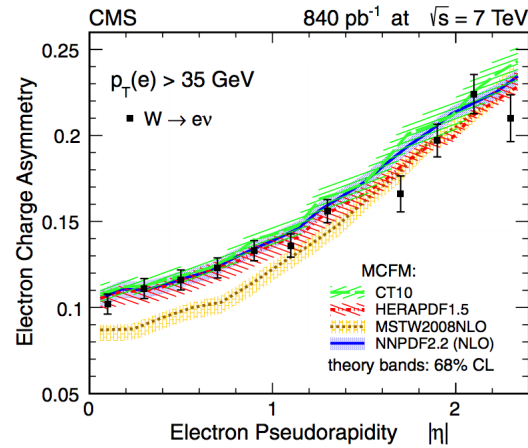


Fig. 14. Lepton charge asymmetry measurement from CMS, using electron channel. With a cut on the electron transverse momentum (35 GeV). The error bars include both statistical and systematic uncertainties.

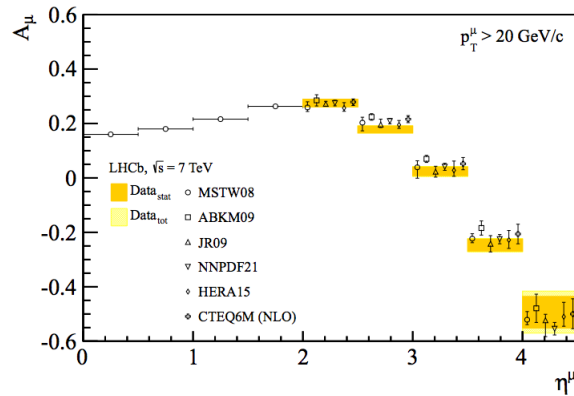


Fig. 15. Lepton charge asymmetry measurement from LHCb. The orange bands correspond to the statistical uncertainties, the yellow bands represent total uncertainty. The measured values are compared with different NNLO predictions.

systematic uncertainty comes from PDFs, which can be possibly suppressed by the update of PDFs sets.

With data corresponding to 2 fb^{-1} of integrated luminosity, CDF performed a measurement of weak mixing angle ³⁶ using $Z \rightarrow ee$ events. Using data corresponding to 4.8 fb^{-1} of integrated luminosity, ATLAS presented a measurement of weak mixing angle ³⁷, after combining both electron and muon channels, the measured

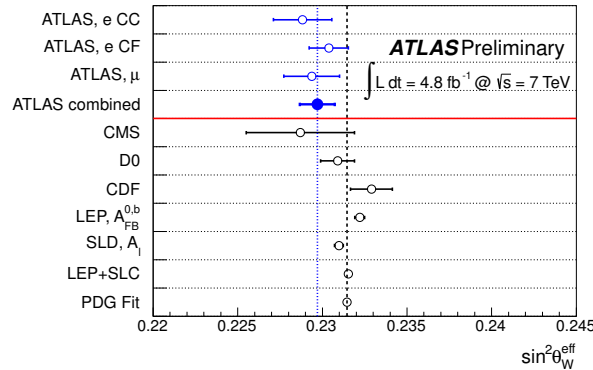


Fig. 16. Comparisons of measured weak mixing angle from different experiments. And the D0 result includes the 90% C.L. PDF uncertainty instead of 68% C.L. PDF uncertainty in other measurements.

value at ATLAS is $0.2297 \pm 0.0004(stat.) \pm 0.0009(syst.)$. The summary for weak mixing angle measurement from different experiments is shown in Fig. 16. The PDF uncertainty is the key element for this measurement at hadron colliders, with more data and new PDF set, the precision of weak mixing angle from hadron collider may be comparable to that from LEP.

5. Summary

Precision measurements with single W and Z bosons events provide stringent tests on the SM. With the data collected from the LHC and Tevatron, good consistency between SM and data is observed, these measurements also provide more information for PDF fitting, critical tests on the high order predictions, and more precisely SM input parameters. With good understanding on the detector response, more precision electroweak results with larger data set will come out soon from both LHC and Tevatron.

6. References

References

1. ATLAS Collab. (G. Aad *et al.*), *JINST* **3**, S08003 (2008).
2. CMS Collab. (S. Chatrchyan *et al.*), *JINST* **3**, S08004 (2008).
3. LHCb Collab. (A. A. Alves Jr. *et al.*), *JINST* **3**, S08005 (2008).
4. CDF Collab. (A. Abulencia *et al.*), *J. Phys. G*, **34**, 2457 (2007).
5. D0 Collab. (V. M. Abazov *et al.*), *Nucl. Instrum. Meth. Phys. Res. A* **565**, 463 (2006).
6. ATLAS Collab. (G. Aad *et al.*), *Phys. Rev. D* **85**, 072004 (2012).
7. CMS Collab., (S. Chatrchyan *et al.*), *J. High Energy Phys.* **007**, 1110 (2011).
8. CMS Collab., (S. Chatrchyan *et al.*), CMS-PAS-SMP-12-011.
9. ATLAS Collab. (G. Aad *et al.*), *Phys. Lett. B* **725**, 223-242 (2013).

10. CMS Collab., (S. Chatrchyan *et al.*), CERN-PH-EP-2013-168.
11. LHCb Collab., (R. Aaij *et al.*) *J. High Energy Phys.* **1206** 058 (2012).
12. LHCb Collab., (R. Aaij *et al.*) *J. High Energy Phys.* **1302** 106 (2013).
13. LHCb Collab., (R. Aaij *et al.*) *J. High Energy Phys.* **1301** 111 (2013).
14. LHCb Collab., (R. Aaij *et al.*) LHCb-CONF-2012-013.
15. D0 Collab., (V. M. Abazov *et al.*), *Phys. Lett. B* **693** 522 (2010).
16. CDF Collab., (T. Aaltonen *et al.*), *Phys. Rev. D* **86** 052010 (2012).
17. CMS Collab., (S. Chatrchyan *et al.*), CMS-PAS-SMP-12-025.
18. D0 Collab., (V. Abazov *et al.*), *Phys. Rev. Lett.* **106** 122001 (2011).
19. A. Banfi, S. Redford, M. Vesterinen, P. Waller, and T. R. Wyatt, *Eur. Phys. J. C* **71**, 3 (2011).
20. ATLAS Collab., (G. Aad *et al.*) *Phys. Lett. B* **720** 32-51 (2013).
21. CDF Collab., (T. Aaltonen *et al.*) *Phys. Rev. D* **108** 151803 (2012).
22. D0 Collab., (V. M. Abazov *et al.*) *Phys. Rev. Lett.* **108** 151804 (2012).
23. CDF and D0 Collab., (T. Aaltonen *et al.*) *Phys. Rev. D* **88** 052018 (2013).
24. ATLAS Collab., (G. Aad *et al.*), *Phys. Rev. D* **85** 072004 (2012).
25. CMS Collab., (S. Chatrchyan *et al.*), *Phys. Rev. Lett.* **109** 111806 (2012).
26. CMS Collab., (S. Chatrchyan *et al.*), *Eur. Phys. J. C* **73** 2318 (2013).
27. S. C. Bennett and C. E. Wieman, *Phys. Rev. Lett.* **82**, 2484 (1999).
28. SLAC E158 Collaboration (P. L. Anthony *et al.*), *Phys. Rev. Lett.* **95**, 081601 (2005).
29. NuTeV Collaboration (G. P. Zeller *et al.*), *Phys. Rev. Lett.* **88**, 091802 (2002) [Erratum-*ibid.* 90, 239902(2003)].
30. LEP Collaborations ALEPH, DEL-PHI, L3 and OPAL; SLD Collaboration, LEP Electroweak Working Group, SLD Electroweak and Heavy Flavor Groups (G. Abbiendi *et al.*), *Phys. Rep.* **427**, 257 (2006).
31. CDF Collaboration (D. Acosta *et al.*), *Phys. Rev. D* **71**, 052002 (2005).
32. D0 Collaboration (V. M. Abazov *et al.*), *Phys. Rev. Lett.* **101**, 191801 (2008).
33. D0 Collaboration (V. M. Abazov *et al.*), *Phys. Rev. D* **84**, 012007 (2011).
34. CMS Collaboration (S. Chatrchyan *et al.*), *Phys. Rev. D* **84**, 112002 (2011).
35. CMS Collaboration (S. Chatrchyan *et al.*), *Phys. Lett. B* **718**, 752 (2013).
36. CDF Collab., (T. Aaltonen *et al.*), *Phys. Rev. D* **88** 072002 (2013).
37. ATLAS Collab., (G. Aad *et al.*), ATLAS-CONF-2013-043.